

PREPARATION AND CHARACTERIZATION OF NANOCRYSTALLINE $\text{Ba}(\text{Ti}_{0.96}\text{Sn}_x\text{Zr}_{0.04-x})\text{O}_3$ CERAMIC

Muazu, A^{1*}, Suleiman, A. B², Abubakar, A.U.³, Zangina, T², Nura, A¹.

¹ Department of Physics, Federal College of Education (T), Bichi, Kano State, Nigeria.

² Department of Physics, Federal University Dutse, Dutse, Jigawa State, Nigeria.

³ Department of Physics, Kano University of Science and Technology, Wudil, Kano State, Nigeria.

*Corresponding Author's Email: hasumm@yahoo.com

ABSTRACT

Nanocrystalline powders of Barium titanate (BaTiO_3 or BT) and $\text{Ba}(\text{Ti}_{0.96}\text{Sn}_x\text{Zr}_{0.04-x})\text{O}_3$ (BTSZ1, BTSZ2, and BTSZ3) [$x=0.02, 0.03$ and 0.04] have been synthesized by a combination of solid-state reaction and high energy ball-milling technique (HBM). The effect of increasing Sn content on the microstructure and dielectric properties of the ceramics were studied. X-ray diffraction patterns show cubic and tetragonal symmetry without secondary phase. Sn^{4+} and Zr^{4+} ions entered the perovskite-type cubic structure and led to an increase in the lattice parameters. The average crystallite size has been calculated using Scherrer formula. Using Scherrer, the crystallite size of the (110) peaks of the pure BT is 31.2 nm and that of BTSZ1, BTSZ2, and BTSZ3 are 42.7, 37.9 and 42.3 nm respectively. The FESEM results indicated a variation of grain size from 144.53, to 89.28 nm for the pure BT, BTSZ1, BTSZ2, and BTSZ3, which show a decrease in grain size as Sn doping increases. Frequency dependence of dielectric permittivity and loss studied in the range temperature and frequency range 30-400°C and 40 Hz–1 MHz, respectively, for BT, BTSZ1, BTSZ2, and BTSZ3 show a normal ferroelectric phase transition behavior. The corresponding dielectric constant and loss at room temperature show that BTSZ2 has the highest dielectric constant and loss of 1671 and 1.6 respectively. The high dielectric constants and relatively lower loss tangent values meet the current demand for device miniaturization in the electronics industry.

Keywords: BT-BTSZ ceramics; high energy ball milling; XRD; FESEM; dielectric properties

1. INTRODUCTION

Barium titanate (BaTiO_3 or BT) is one of the most basic and widely applied ferroelectric oxide materials with a perovskite- ABO_3 type crystalline structure. Due to its excellent dielectric, ferroelectric, piezoelectric, pyroelectric and optoelectronic properties it is extensively used in multilayer ceramic capacitors (MLCC), positive temperature coefficient of resistance (PTCR) thermistors, piezoelectric sensors, actuators (Yu *et al.*, 2000; Zhao *et al.*, 2003; Markovic *et al.*, 2009; Wang *et al.*, 2010), ferroelectric random access memories (FRAM) (Uchino *et al.*, 2000) and electro-optic devices (Haertling *et al.*, 1999). It is well known that as the grain size of BT ceramics is reduced to the micron level, the permittivity at room temperature increases. Further reduction in grain size to less than few hundred nanometers leads to a permittivity decrease (Hoshina *et al.*, 2008). Modified barium titanate compositions are widely used in MLCCs due to their high dielectric constant and low loss (Jaffe *et al.*, 1971). Among the doped BT compositions, $\text{Ba}(\text{Ti}_{1-x}\text{Sn}_x)\text{O}_3$ (BST) system has drawn wide attention due to their manifestation of diffuse-type phase transition (Xiaoyong *et al.*,

2003; Lu *et al.*, 2004; Wei *et al.*, 2007) It is known that the cubic-tetragonal phase transition displays a continuous crossover with increase in the content of Sn from a sharp ferroelectric phase transition to a diffused phase transition and towards a relaxor-type behavior. On the other hand, the Zr addition in BZT lowers the dielectric loss due to its larger ionic size which expands the perovskite lattice whereas increase in its concentration induces a reduction in the average grain size, decreases the dielectric permittivity (ϵ_r) enabling it to maintain a low and stable leakage current (Rehrig *et al.*, 1999; Zhi *et al.*, 2000 and 2001). The Curie temperature of barium titanate system can be altered by the substitution of dopants into either A- or B-site. Partial replacement of titanium by tin, zirconium, or hafnium generally leads to a reduction in T_c and an increase in the permittivity maximum (ϵ_{max}) with dopant content (Hennings *et al.*, 1982). Therefore, co-doping BT with two tetravalent ions Sn^{4+} and Zr^{4+} would be a good strategy to tailor the properties of BT ceramics.

As technological advances demand more complex portable devices with various functions, the fabrication of thinner dielectric layers of MLCCs become a more significant issue as these devices become more miniaturized. Therefore, it is necessary to use powders of ferroelectric compounds with small grain size (submicron or even nanosize) and narrow size distribution. Hence, mechanochemical synthesis via high energy ball-milling (HBM) technique is employed here to reduce grain size of doped BT to nanosize. HBM ball-milling technique is still considered a simple and cost effective method for large scale production of nanoceramic powders (Jiang *et al.*, 1998; Wang *et al.*, 2007) as the method is superior to both conventional solid-state reaction and wet-chemistry-based processing routes for several reasons. These include low-cost and widely available oxides as starting materials, whereas wet chemical routes are extremely sensitive to environmental conditions such as moisture, light and heat. The objective of this work is to study the structural, and dielectric properties of mechanochemically synthesized BT and Sn/Zr doped BT ceramics.

2. Experimental Procedure

Synthesis of Barium titanate and Zirconium and tin doped Barium titanate

BT and $\text{Ba}(\text{Ti}_{0.96}\text{Sn}_x\text{Zr}_{0.04-x})\text{O}_3$ ($x = 0.02, 0.03$ and 0.04) nanocrystalline powders were synthesized by a combination of solid state reaction and high energy ball-milling technique (HBM). The starting materials were analytical grade oxide precursors, BaCO_3 ($\geq 99\%$, Merck, Germany), TiO_2 (99.9%, Aldrich, U.S.A), ZrO_2 (99%, STREM, U.S.A and SnO_2 (99.9%, STREM, U.S.A). Stoichiometric amounts of the oxides were weighed according to

the nominal composition and ball-milled for 12 h in alcohol. The notations and formulas of the selected compositions of BTSZ solid solution are shown in Table 1. The mixture was dried in an oven and calcined in an alumina crucible at 1050°C for 4 h in air to yield BT and Ba (Ti_{0.96}Sn_xZr_{0.04-x})O₃ ceramics where x= 0.02, 0.03 and 0.04.

The calcined powders were ball- milled in an isopropyl alcohol as wetting medium using SPEX 8000 Mixer/Mills for 7 h at room temperature. The milling was stopped for 15 min after every 60 min of milling to cool down the system. The slurry was put in oven and dried at 90°C for 24 h. The milled powder was compacted at 49033.25 N/m² to make pellets of size 10 mm in diameter and 1 mm thickness using polyvinyl alcohol (PVA) as a binder. The pellets were sintered in a programmable furnace at temperatures of 1190°C for 2 h in alumina crucibles.

Characterization:

- Structural properties were obtained using X-ray diffractometer (XPRT-PRO) with monochromatic Cu K α radiation at $\lambda = 1.54178 \text{ \AA}$ at 40 kV/40 mA in the 2 θ range from 20° to 80°. The experimental densities of the samples were calculated using Archimedes principle. The morphological studies of the sintered sample were carried out using field emission scanning electron microscopy (FESEM, JEOL 7600F, U. S. A), operated at a voltage of 15 kV and images captured at 5 kV with magnification of 100,000.
- The dielectric properties of the ceramics were evaluated using Impedance Analyzer (Agilent 4294A, Japan) using an amplitude of 500 mV in the frequency and temperature range of 40 Hz – 1M Hz and 30 to 400°C respectively.

Table 1: Compositions of BTSZ solid solution

Samples	Description
BT	BaTiO ₃
BTSZ1	Ba (Ti _{0.96} Sn _x Zr _{0.04-x}) O ₃ , x = 0.02
BTSZ2	Ba (Ti _{0.96} Sn _x Zr _{0.04-x}) O ₃ , x = 0.03
BTSZ3	Ba (Ti _{0.96} Sn _x Zr _{0.04-x}) O ₃ , x = 0.04

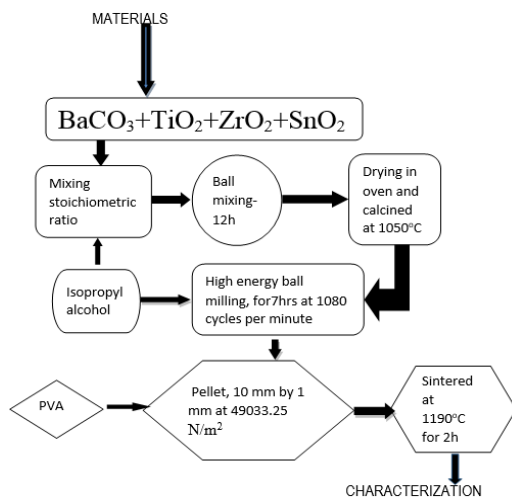


Fig. 1: A Flowchart of the synthesis of BT, BTSZ1, BTSZ2 and BTSZ3 by using a combination of solid state reaction and high-energy ball milling.

3. Result and Discussion

3.1. XRD Analysis

Fig. 2 shows the room temperature XRD patterns of BT, BTSZ1, BTSZ2 and BTSZ3 ceramics. The enlarged XRD patterns of the ceramics in the range of 2 θ from 44 to 46.5° clearly show that the crystal structure of the ceramic is cubic for BT with space group *P m -3 m*, because the (200) and (002) peaks are not split (Buttner *et al.*, 1992), whereas it is tetragonal for BTSZ1, BTSZ2 and BTSZ3 with the splitting of the (200) and (002) characteristic peaks at 2 θ of 45.2°, 45.3°, and 45.16°. The positions of the diffraction peaks of the ceramics shift slightly to lower angle with increase of Sn. The lattice constant of all the samples are estimated using the equations.

$$\text{For cubic phase, } a = b = c \quad a^2 = \frac{\lambda [(h^2+k^2+l^2)]}{2 \sin^2\theta} \quad (1)$$

$$\text{For tetragonal phase, } a = b \neq c \quad \frac{1}{d_{hkl}^2} = \frac{1}{a^2} (h^2 + k^2) + \frac{l^2}{c^2} \quad (2)$$

where λ is the wavelength of X-ray ($\lambda = 1.54178 \text{ \AA}$), θ is the Bragg angle and hkl are the Miller indices of the corresponding planes. To calculate c , those (hkl) values for which $h = k = 0$ and $l \neq 0$ have been used.

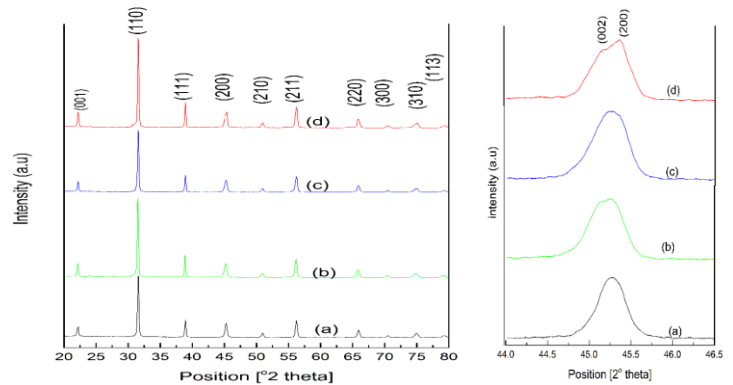


Fig. 2: XRD Patterns of (a). BT (b). BTSZ1 (c). BTSZ2 and (d). BTSZ3 sintered at 1190°C

3.2. Crystal Size Measurements

The crystal size for BT and BTSZ samples was calculated from the full width at half maximum (FWHM) of the (110) by using the Debye Scherrer equation (Scherrer 1918).

$$D = \frac{0.98\lambda}{\beta \cos\theta} \quad (3)$$

where D is the crystallite size, 0.9 is the crystalline shape factor, λ is the X-ray wavelength of CuK α ($\lambda = 1.54178 \text{ \AA}$), β is the full width at half maxima (FWHM) at Bragg's angle (2θ).

The result of the calculation of the lattice parameters, crystallite size, and unit cell volume of BT and BTSZ ceramic sintered at 1190°C for 2 h are shown in Table 2. As the Sn content increases from BTSZ1 to BTSZ2, the a -lattice constant decreases whereas the c -lattice increases with a corresponding increase of the tetragonality of the system. With further increase of Sn in BTSZ3, both the lattice constant and tetragonality increases. The crystal

cell volumes for BT, BTSZ1, BTSZ2, and BTSZ3 were determined to be 64.254, and 64.398, 64.386, 64.448 Å³, respectively.

Table 2: Structural parameters of BT and BTSZ ceramics sintered at 1190°C for 2 h.

Sample	FWHM(°)	2θ°	a (Å)	b(Å)	c (Å)	c/a	Volume (Å ³)	Crystal size nm
BT	0.2647	31.5427	4.00522	4.00522	4.00522	1.00000	64.254	31.21
BTSZ1	0.1933	31.4781	4.00190	4.00190	4.02107	1.00478	64.398	42.73
BTSZ2	0.2176	31.5212	4.00141	4.00141	4.02115	1.00492	64.386	37.96
BTSZ3	0.1951	31.5280	4.00260	4.00260	4.02264	1.00498	64.448	42.34

3.3. Surface morphology

FESEM micrographs of BT, BTSZ1, BTSZ2 and BTSZ3 ceramics shown in Fig. 3 reveal dense and non-uniform microstructures with presence of void. The average grain size of BT, BTSZ1, BTSZ2 and BTSZ3 ceramics are listed in Table 3. The grain size increases from 144.53 nm at BT to 199.65nm at BTSZ1 and decrease to 89.28nm with increase in Sn concentration. A decrease of grain size can be observed in Table 3 which indicates that Sn is a grain growth inhibitor. The increase of experimental, relative density and decrease of porosity (Table 3) with Sn concentration enhances the density of the ceramics with reduction of pores.

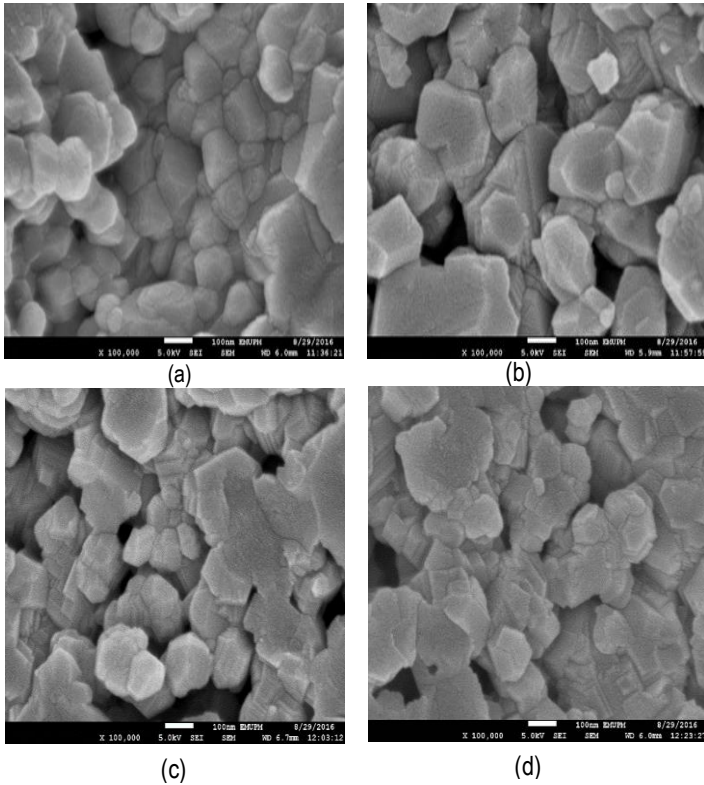


Fig. 3: FESEM images at magnification of 200,000 of nanocrystalline samples of: (a) BT (b) BTSZ1 (c) BTSZ2 and (d). BTSZ3 sintered at 1190°C.

The experimental density was calculated using the formula:

$$\rho_{exp} = \frac{M_a \rho_w}{M_a - M_w} \tag{4}$$

where M_a and M_w are the respective weight in gram of the pellet measured in air and in distilled water and ρ_w is the density of pure water in g/cm³.

The theoretical density of the material is calculated by using formula,

$$\rho = \frac{cell\ mass}{cell\ volume} = \frac{n \times M \times 1.66 \times 10^{-24}}{V} g/cm^3, \tag{5}$$

where n is the number of atoms per unit cell, M is the molecular weight of atoms constituting one unit of the chemical formula, and V is the unit cell volume obtained from lattice parameters. The calculated values of theoretical density, experimental density, relative density, porosity and grain size are shown in Table 3.

The decrease of crystallite size of BTSZ1to BTSZ2 from 42.37 to may be attributed to decrease of Zr concentration to 0.01 as the radius of Zr⁺⁴ (0.72 Å) is greater than that of Sn⁺⁴ (0.69 Å). In general, at normal temperature bulk barium titanate exists in ferroelectric phase, however due to microstructural size effect nanocrystals of barium titanate are stable in cubic phase (Hsiang *et al.*, 1996). With the doping of Sn and Zr ions on B site, the resultant displacement of Sn, Zr, Ti ions and O₂ increase and distorts the shape of cell. The c-axis along which displacement takes place elongated and the other two axes a and b-axis shortened, and the cubic crystalline structure turns in to tetragonal, hence, the increase of c-axis, (a/c) and decrease of a-axis with increase of Sn concentration, respectively (Table 1). Another explanation is that the bigger Zr⁴⁺ ions occupy the Ti site and then the c-axis lattice constant is increased.

Table 3: Various observed parameters of BT and BTSZ ceramics

Sample	Theoretical density (ρ _{th}) (g/cm ³)	Experimental density (ρ _{exp})(g/cm ³)	Relative density (%)	% Porosity	Grain size nm
BT	6.02	5.639	93.6	6.34	144.53
BTSZ1	6.17	5.382	87.2	12.77	199.65
BTSZ2	6.19	5.418	87.5	12.47	84.54
BTSZ3	6.18	5.502	89.0	10.97	89.28

3.4. Dielectric properties

The real (ε') part of relative permittivity and tan δ within the frequency range of 40 Hz - 1 MHz of BT, BTSZ1, BTSZ2 and BTSZ3 ceramics at room temperature are shown in Fig. 4 and 5 respectively. The value of dielectric constant is higher at lower frequency and decreases with increase in frequency due to the dielectric relaxation, which is a characteristic feature of the ferroelectric materials irrespective of composition of the specimens (Lines *et al.*, 1979). The values of real dielectric constant and loss tangent for BT and BTSZ1, BTSZ2 and BTSZ3 are shown in table 3.

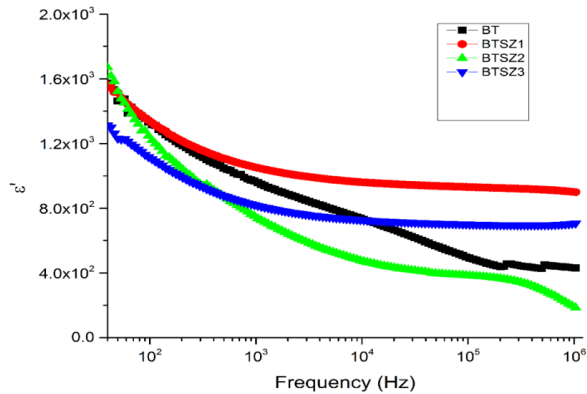


Fig. 4: Variation of real part of relative permittivity (ϵ') of nanocrystalline BT, BTSZ1, BTSZ2 and BTSZ3 ceramics at 30°C.

Fig. 5 is a plot of the frequency dependence of dielectric loss ($\tan \delta$) of BT, BTSZ1, BTSZ2 and BTSZ3 at various temperatures. Similar to the behavior of ϵ' with frequency, the dielectric loss exponentially decreases with decreasing frequency to almost zero for BT and BTSZ3 but rises beyond 10^5 Hz for BTSZ1 and BTSZ2 sample respectively.

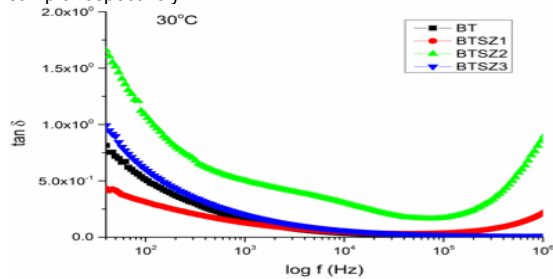


Fig. 5: Variation of loss tangent with frequency of nanocrystalline BT, BTSZ1, BTSZ2 and BTSZ3 ceramics at 30°C.

The best sample is BTSZ2 because it exhibited high dielectric permittivity of 1671 even though it has slightly higher loss of 1.6 among the samples. This shows the importance of this material for MLCC and energy storage applications.

Frequency dependent dielectric permittivity (ϵ') and loss factor ($\tan \delta$) of BT, BTSZ1, BTSZ2 and BTSZ3 nanocrystalline ceramics at 50 to 150°C are shown in Fig. 6 and 7. In Fig. 7(b) there is generally an increase in ϵ' with increase in Sn content which become almost constant at the lower frequency region up to about 10^5 Hz, then decreased with increase of frequency and temperature. Low dispersion of dielectric constant from 50 to 150°C for BTSZ2 and BTSZ3 samples are shown in Fig. 6(c) and (d) the ϵ' decreases with increase of frequency and temperature. It appeared to have lost its frequency dependence at higher frequencies, because the interfacial polarization is insignificant at high frequencies and hence ϵ' remains relatively constant.

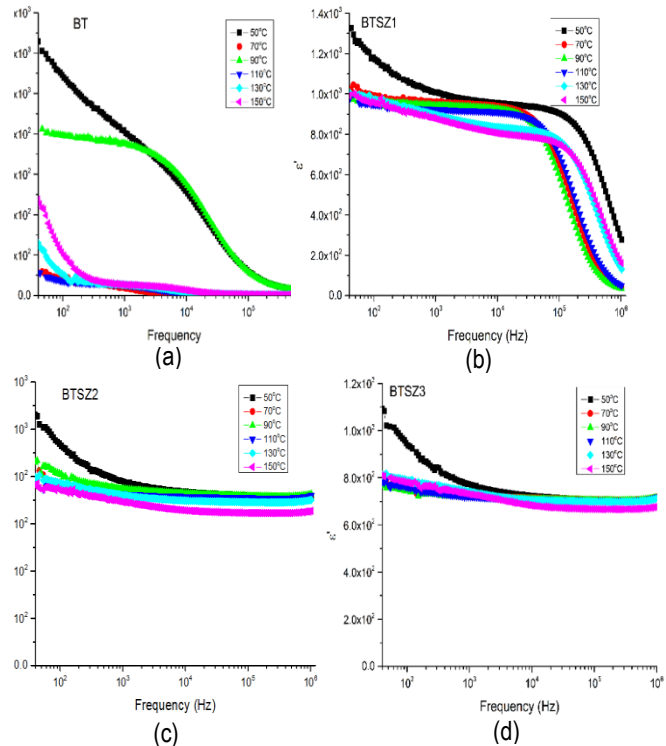
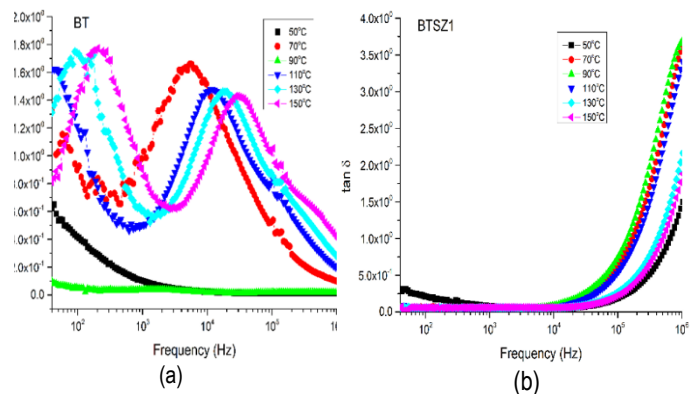


Fig.6 Frequency dependences of real part of relative permittivity nanocrystalline ceramic at various temperature: (a) BT, (b) BTSZ1, (c).BTSZ2 and (d). BTSZ3

Fig. 7(a-d) shows the frequency dependences of dielectric loss of nanocrystalline BT, BTSZ1, BTSZ2 and BTSZ3 ceramic at 50 to 150°C. The $\tan \delta$ of BT is depicted in Fig. 7(a) at 70°C and 110-150°C there is dispersion at low frequency with two relaxation peaks. In Fig. 9b $\tan \delta$ increase beyond 10^4 and 10^5 Hz at all the temperatures.



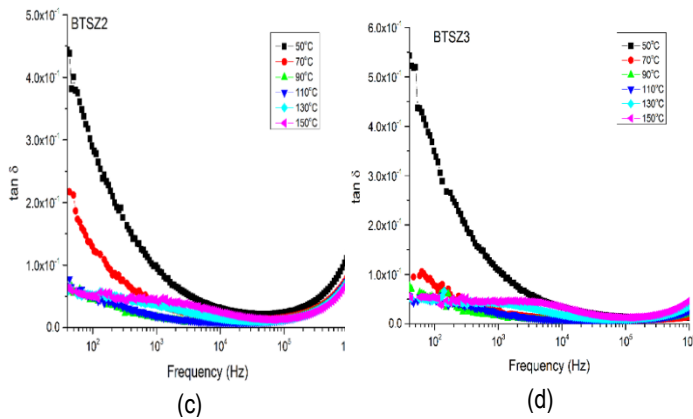


Fig. 7: Frequency dependences of dielectric loss of nanocrystalline ceramic at various temperature: (a). BT, (b) BTSZ1, (c) BTSZ2 and (d) BTSZ3

The variation of dielectric constant and tangent loss as a function of temperature for BT, BTSZ1, BTSZ2 and BTSZ3 ceramics measured from room temperature to 150°C at the frequency of 100 Hz is shown in Fig. 8(a) and (b), respectively. From Fig. 8(a) the maximum dielectric constant of BT, BTSZ1, BTSZ2 and BTSZ3 is at room temperature and decreases with increase in temperature. The dielectric constant of BT decreased from 30°C to 70°C and then increased sharply at 90°C. Thereafter, it fall to the lowest level at 110°C, thus indicating a phase transition. For BTSZ samples, the phase transition seems to be shifted towards lower room temperature with increase in doping concentration as reported by other workers (Alkathya *et al.*, 2016).

In Fig. 8b the dielectric loss beyond 70°C becomes almost independent and later merges at higher temperature, except for BT which rapidly increases with increase in temperature beyond 90°C. From Fig. 8a the phase transition shows the diffuse transition behavior. This diffuseness in phase transition can be clarified by the tolerance factor (*t*). The calculated tolerance factor is equal to 1.0584, 1.0585 and 1.0587 for BTSZ1, BTSZ2 and BTSZ3 respectively. The decreases of "*t*" value indicated that the ferroelectric phase-transition occur at much lower temperature.

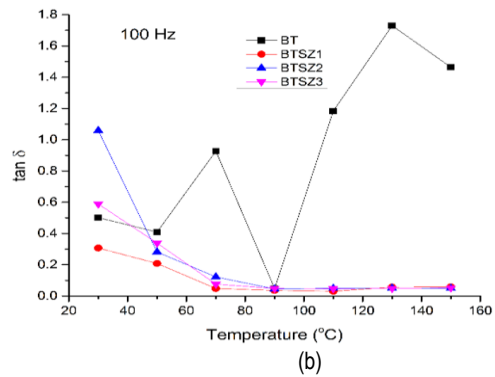
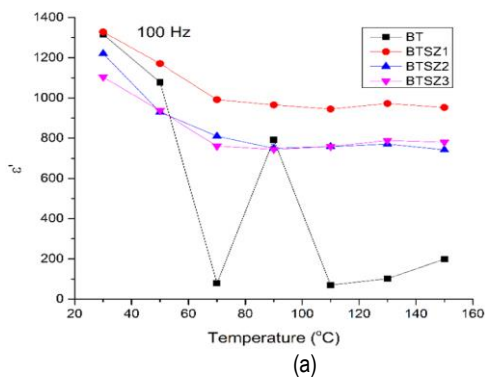


Fig. 8: Variation of (a) dielectric constant and (b) loss tangent with temperature at 100 kHz for BT, BTSZ1, BTSZ2 and BTSZ3 nanocrystalline ceramic.

4. Conclusion

Nanocrystalline BT, BTSZ1, BTSZ2 and BTSZ3 samples has been prepared by combination of solid state and high energy ball milling technique. X-ray analysis confirms the cubic and tetragonal perovskite structure at room temperature. FESEM images show samples are dense and have uniform microstructures with certain amount of porosity. The grain size tends to decrease from 144.53 to 89.28 nm with increase in Sn content. The frequency dependence dielectric study reveals a normal ferroelectric behavior in the material. Room-temperature dielectric constant increases with the Sn and Zr substitution while dielectric loss decreases. Increase in Sn amount increases the crystal tetragonality, which results in increased polarization and the relative dielectric permittivity. The Curie temperature (*T_c*) of BT is found to be 90°C, while BTSZ samples do not manifest any sign of a phase transition implying that its *T_c* may be below room temperature with doping concentration. The composition BTSZ2, exhibited high real relative dielectric permittivity with dielectric loss of 1671 and 1.6 respectively at room temperature, hence the best candidate for MLCCs and energy storage application.

Acknowledgements

The authors gratefully acknowledge the Physics Department, Faculty of Science, UPM, Malaysia for providing support and facilities to carry out structural and electrical measurements.

REFERENCES

Alkathya, M.S., Joseph, A. and Raju, K.C.J. (2016). Dielectric Properties of Zr substituted Barium Strontium Titanate. *Materials Today: Proceedings* 3, 2321–2328

Buttner, R. H., Maslen, E. N., *Acta Crystallographica Section B*, **48**, 764 - 769, (1992).

Haertling, G. H., (1999). Ferroelectric ceramics: history and technology. *Journal of American Ceramic Society*, **82** (4): 797-818.

Hennings, D., Schnell, A. and Simon, G. (1982). Diffuse Ferroelectric Phase Transitions in Ba (Ti_{1-y}Zr_y) O₃ Ceramics, *Journal of American Ceramic Society*, 65,539.

Hoshina, T., Takizawa, K., Li, J., Kasama, T., Kakemoto, H., and Tsurumi, T. (2008). *Journal of the Physical Society of Japan*, **47**, 76077611

Hsiang, H-I., Yen, F-S., Chang, Y. H. (1996). "Effects of doping with

- La and Mn on the crystallite growth and phase transition of BaTiO₃ powders", *Journal of Material Science*, 31, 2417–2424
- Jaffe, B., and Cook, W R., Jaffe, H. (1971). Piezoelectric ceramics, Academic Press Limited, London,
- Jiang, A. Q., Li, H. G., Zhang, L. D. (1998). Dielectric study in nanocrystalline Bi₄Ti₃O₁₂ prepared by chemical coprecipitation. *Journal of Applied Physics*, 83, 4878, <https://doi.org/10.1063/1.367287>
- Lines, M. E., Glass, A. M. (1979). Principles and applications of ferroelectrics and related materials, Oxford, Clarendon.
- Lu, S.G., Xu, Z.K., and Chen, H. (2004). Tunability and relaxor properties of ferroelectric barium stannate titanate ceramics. *Applied Physics Letters*, 85(22):5319-5321.
- Markovic, S., Miljkovic, M., Jovalekic, C., Mentus, S., Uskokovic, D. (2009). Densification, microstructure, and electrical properties of BaTiO₃ (BT) ceramics prepared from ultrasonically de-agglomerated BT powders. *Materials and Manufacturing Processes*, 24, 1114–1123.
- Rehrig, P. W., Park, S. E., McKinstry, S. T., Messing, G. L., Jones, B., Shrout, T. M. (1999). *Journal of Applied Physics*, 86, 1657 Soc., 72 1355.
- Scherrer, P., *GottingerNachrichten*. 2(1918) 98.
- Uchino, K. (2000). *Ferroelectric Devices*, Marcel Dekker, New York.
- Wang, J.F., Pu, Y.P., Yang, G.G., Chen, X.L. (2010). Characteristics of the PTCR in high- curie-point lead-free barium titanate ceramics and their grain structures. *Materials and Manufacturing Processes*, 25,707–709.
- Wang, Y., Li, Y., Rong, C., Liu, P. (2007). *Journal of Nanotechnology*, 18, 465701
- Wei, X., and Yao, X. (2007). Preparation, structure and dielectric property of barium stannate titanate ceramics, *Material and Science Engineering B* 137,184-188
- Xiaoyong, W., Yujun, F., Xi, Y. (2003). *Applied Physics Letters*, 83, 2031
- Yu, Z., Guo, R. A. and Bhalla, S. (2000). *Journal of Applied Physics*, 88, 410–415
- Zhao, J., Li, L., Wang, Y., and Gui, Z. (2003). DC Bias Properties of Ba_{1-x}Sr_xTiO₃ Ceramics. *Material and Science Engineering*, B99, 207–210.
- Zhi, Y., Guo, R., Bhalla, A. S. (2000). *Journal of Applied Physics*, 88,410
- Zhi, Y., Guo, R., Bhalla, A. S. (2001). *Journal of Crystal Growth*, 233,460